Development 137, 2365-2374 (2010) doi:10.1242/dev.047605

Myocardin-related transcription factors regulate the Cdk5/Pctaire1 kinase cascade to control neurite outgrowth, neuronal migration and brain development

Maysa H. Mokalled, Aaron Johnson, Yuri Kim, Jiyeon Oh and Eric N. Olson*

SUMMARY

Numerous motile cell functions depend on signaling from the cytoskeleton to the nucleus. Myocardin-related transcription factors (MRTFs) translocate to the nucleus in response to actin polymerization and cooperate with serum response factor (Srf) to regulate the expression of genes encoding actin and other components of the cytoskeleton. Here, we show that MRTF-A (Mkl1) and MRTF-B (Mkl2) redundantly control neuronal migration and neurite outgrowth during mouse brain development. Conditional deletion of the genes encoding these Srf coactivators disrupts the formation of multiple brain structures, reflecting a failure in neuronal actin polymerization and cytoskeletal assembly. These abnormalities were accompanied by dysregulation of the actin-severing protein gelsolin and Pctaire1 (Cdk16) kinase, which cooperates with Cdk5 to initiate a kinase cascade that governs cytoskeletal rearrangements essential for neuron migration and neurite outgrowth. Thus, the MRTF/Srf partnership interlinks two key signaling pathways that control actin treadmilling and neuronal maturation, thereby fulfilling a regulatory loop that couples cytoskeletal dynamics to nuclear gene transcription during brain development.

KEY WORDS: Neurite outgrowth, Neuronal migration, MRTF, Pctaire1 (Cdk16), Actin dynamics, Mouse

INTRODUCTION

Precisely controlled neuronal migration and neuronal connectivity establish normal brain architecture and maintain neurological and cognitive functions (Ayala et al., 2007; Lin et al., 2009). Aberrant neuronal migration or connectivity causes multiple neurodevelopmental and neurodegenerative disorders, including mental retardation, schizophrenia and Alzheimer's disease. Although these disorders differ in their onsets and pathologies, they share common etiologies, including the absence of functional neurons in discrete regions of the brain, decreased neurite arborization and weak synapse connections. Elucidating the molecular pathways that control neuronal survival, migration and connectivity represents an important step towards the identification of novel therapeutic targets to enhance neuronal function in these brain disorders (Benitez-King et al., 2004; Lin et al., 2009; Spalice et al., 2009; Verrotti et al., 2009).

Neurons originate in the ventricular zones of the brain and undergo stereotypical migration to populate specific brain structures. Neuronal migration depends on neurite extension and outgrowth, during which neurons dynamically generate and retract growth cones in search of extracellular guidance cues (Ayala et al., 2007; Lambert de Rouvroit and Goffinet, 2001). Several extracellular guidance molecules, cell-adhesion complexes and neurotrophic factors regulate neurite outgrowth and instruct directional neuronal migration during neurogenesis and in the adult brain (Ayala et al., 2007; Rossi et al., 2007; Lin et al., 2009; Park et al., 2002).

Dynamic changes in the actin cytoskeleton provide the mechanical force for neurite outgrowth and migration. Regulation of actin polymerization is crucial to shape and direct growth cones during neurite outgrowth and requires a pool of monomeric G-actin to extend filamentous F-actin fibers towards the leading edge of the outgrowth. Guidance molecules orchestrate directional cell movement by regulating the transcription of genes encoding actin and other cytoskeletal components and the activity of cytoskeletal regulatory proteins such as the F-actin-severing proteins gelsolin and cofilin (Cunningham et al., 1991; Furnish et al., 2001; Lin et al., 2009; Meberg, 2000; Meberg and Bamburg, 2000; Park et al., 2002; Stern et al., 2009; Tanaka et al., 2008). The intracellular pool of available G-actin governs the rate of actin polymerization and is regulated at both the transcriptional and post-transcriptional levels by extracellular signals. However, the intracellular regulatory cascades that sense G-actin levels and provide the appropriate intracellular response to guidance cues remain poorly understood.

Members of the myocardin family of transcription factors modulate cytoskeletal dynamics by sensing actin polymerization and conferring transcriptional activity to serum response factor (Srf) (Olson and Nordheim, 2010). The myocardin family includes myocardin and the myocardin-related transcription factors (MRTFs) -A and -B (also known as Mkl1 and Mkl2 – Mouse Genome Informatics). Unlike myocardin, which is expressed specifically in cardiac and smooth muscle (Oh et al., 2005; Wang et al., 2001; Wang et al., 2002), the expression of MRTF-A and MRTF-B is enriched in the forebrain, particularly in the hippocampus and cerebral cortex (Alberti et al., 2005; Shiota et al., 2006). Studies in fibroblasts and muscle cells show that MRTFs bind monomeric G-actin in the cytoplasm and translocate into the nucleus in response to signals promoting actin polymerization to form powerful transcriptional complexes with Srf (Guettler et al., 2008; Kuwahara et al., 2005; Miralles et al., 2003; Pipes et al., 2006; Posern et al., 2004; Vartiainen et al., 2007).

Mouse embryos homozygous for an *Srf*-null mutation fail to generate mesoderm and die at gastrulation (Arsenian et al., 1998); however, tissue-specific deletion of *Srf* has revealed multiple roles for this transcription factor in brain, muscle, heart and liver

Department of Molecular Biology, UT Southwestern Medical Center at Dallas, 5323 Harry Hines Boulevard, Dallas, TX 75390-9148, USA.

*Author for correspondence (eric.olson@utsouthwestern.edu)

Accepted 11 May 2010

development (Charvet et al., 2006; Latasa et al., 2007; Miano et al., 2004; Niu et al., 2005; Parlakian et al., 2005). Conditional deletion of *Srf* in the brain impairs neurite outgrowth, axon guidance and directional neuron migration (Alberti et al., 2005; Knoll et al., 2006). Deletion of *Srf* in the brain also disrupts the formation of hippocampal neuronal circuitry, resulting in defective memory formation. *Srf*-null CA1 pyramidal neurons display diminished long-term synaptic potentiation (LTP) and impaired induction of long-term synaptic depression (LTD), indicating that Srf is required for plastic modification of synaptic strength in response to activity in the adult brain (Etkin et al., 2006; Ramanan et al., 2005). However, mice lacking any single member of the myocardin family fail to phenocopy *Srf* loss-of-function mutations. *Mrtfa* knockout mice have defects in mammary myoepithelial cell differentiation but appear otherwise normal (Li et al., 2006; Sun et al., 2006), whereas global deletion of *Mrtfb* causes defects in the patterning of the branchial arch arteries and post-gastrulation embryonic lethality (Li et al., 2005; Oh et al., 2005). These studies suggest either that in vivo Srf activity relies on transcriptional co-factors outside of the myocardin family or that functional redundancy among MRTF members obscures individual gene functions.

Here, we show that a single allele of either *Mrtfa* or *Mrtfb* is sufficient to support normal brain development; however, brain-specific deletion of *Mrtfb* in *Mrtfa*-null mice causes lethality between postnatal day (P) 16 and 21. Mice lacking both *Mrtfa* and *Mrtfb* in the brain show several morphological abnormalities that phenocopy the defects reported for brain-specific deletion of *Srf* (Alberti et al., 2005; Knoll et al., 2006). The morphological defects in *Mrtfa/b* mutant mice are accompanied by aberrant neuronal migration, impaired neurite outgrowth and decreased expression and activity of actin and the actin-severing proteins gelsolin and cofilin. We also identify the gene encoding Pctaire1 kinase as a novel target of the MRTF/Srf pathway in the brain. Pctaire1 links MRTF/Srf signaling to the Cdk5 pathway, a known regulator of actin dynamics that promotes neuronal migration and neurite outgrowth. We conclude that MRTF-A and MRTF-B are key molecular sensors in a tightly controlled regulatory feedback loop that links extracellular signaling and cytoskeletal activity with Srf transcriptional regulation to modulate actin dynamics during brain development in vivo.

MATERIALS AND METHODS

Mouse lines

The *Mrtfb* conditional null allele was generated using homologous recombination in embryonic stem (ES) cells. The pGKNEO-F2L2DTA vector, which contains a neomycin resistance gene flanked by FRT and loxP sites and a diphtheria toxin gene cassette, was used for *Mrtfb* targeting. The 5′ arm, knockout arm and 3′ arm of the targeting construct were generated by high-fidelity PCR amplification (Expand High-Fidelity Long Template, Roche) of 129SvEv genomic DNA. The targeting vector was linearized with *Pvu*I and electroporated into 129SvEv-derived ES cells. Isolated ES cell clones were analyzed for homologous recombination. Incorporation of the 5′ and 3′ loxP sites was confirmed by Southern blotting using 5′ and 3′ probes following digestion with *Xba*I and *Sac*I, respectively. Clones with the targeted *Mrtfb* allele were injected into 3.5-day C57BL/6 blastocysts, and the resulting chimeras were crossed to C57BL/6 females to achieve germline transmission of the targeted ($Mrtfb^{neo\text{-}loxP}$) allele. The $Mrtfb^{neo\text{-}loxP}$ mice were crossed to *FLPe* transgenic mice, then to *GFAP-Cre* transgenic mice (Zhuo et al., 2001) to obtain the $Mrtfb^{F}$ and $Mrtfb^{KO}$ alleles, respectively. $Mrtfb^{F/F}$;*GFAP-Cre* mice were then crossed to $Mrtfa^{-/-}$ mice (Li et al., 2006) to generate $Mrtfa^{-/-}$;$Mrtfb^{F/F}$;*GFAP-Cre* (MRTF bdKO) mice. *Srf* heterozygous mice (Arsenian et al., 1998) were used as controls.

Histology and Immunohistochemistry

Control and bdKO mice were anesthetized and transcardially perfused with PBS, followed by 4% paraformaldehyde (PFA) prior to brain dissection. Brains were then postfixed in 4% PFA for 2 days, embedded in paraffin and sectioned. Sections were stained with Hematoxylin and Eosin, Nissl stain, or phalloidin stain using standard procedures. TUNEL assay and Golgi staining were performed according to manufacturers' instructions (Roche and FD Neurotechnologies, respectively). Immunohistochemistry using monoclonal anti-BrdU (Roche), monoclonal anti-MAP2 (Sigma), anti-Pctaire1 (Santa Cruz Biotechnology), anti-phospho-Cdk5 (Santa Cruz Biotechnology), anti-phospho-Pak (Cell Signaling), anti-phospho-LimK (Abcam), anti-phospho-cofilin (Sigma), anti-β-tubulin J1 (Tubb3) (Abcam) and anti-Gfap (Sigma) antibodies was performed using standard protocols.

BrdU labeling

Timed matings were set up between $Mrtfa^{-/+}$;$Mrtfb^{F/F}$ female and $Mrtfa^{-/+}$;$Mrtfb^{F/F}$;*GFAP-Cre* male mice. Pregnant females were intraperitoneally injected with BrdU (Roche; 100 μg/g body weight) at embryonic day (E) 15.5. The pups were genotyped and sacrificed at P7. $Mrtfa^{-/-}$;$Mrtfb^{F/F}$;*GFAP-Cre* and $Mrtfa^{-/+}$;$Mrtfb^{F/F}$ control brains were sectioned for Hematoxylin and Eosin staining and for BrdU labeling.

Neurite outgrowth assay

$Mrtfa^{-/-}$;$Mrtfb^{F/F}$ and $Mrtfa^{-/+}$;$Mrtfb^{F/F}$ mouse pups (P0-P3) were used for hippocampal and cortical cultures as described (Ahlemeyer and Baumgart-Vogt, 2005). The cultures were plated on poly-D-lysine/laminin-coated coverslips (BD Biosciences) and infected with either Ad5CMVCre-eGFP or Ad5CMVeGFP adenovirus constructs (University of Iowa Gene Transfer Vector Core). After 2 weeks, the cells were fixed with 4% PFA, permeabilized and blocked with 3% bovine serum albumin in PBST buffer (PBS containing 0.1% Tween 20). The cells were then incubated with anti-MAP2 primary antibody (1:500 in PBST) for 45 minutes followed by three washes in PBST and incubation with Texas-Red-conjugated secondary antibody. After three washes in PBST, coverslips were mounted on glass slides using VectaShield mounting medium with DAPI (Vector Laboratories) and visualized with a confocal microscope.

RT-PCR analysis

Total RNA was purified from tissues using TRIzol reagent according to the manufacturer's instructions (Invitrogen). For RT-PCR, total RNA was used as a template for reverse transcription (RT) using random hexamer primers. Quantitative real-time PCR (qPCR) was performed using TaqMan probes (ABI).

Western blots

Cortical brain tissues were homogenized in lysis buffer (50 mM Tris pH 7.4, 150 mM NaCl, 1% Triton X-100, 1 mM EDTA) supplemented with protease inhibitors (Complete Mini, EDTA-free, Roche) and phosphatase inhibitors (Sigma). The lysates were then centrifuged at 14,000 ***g*** for 15 minutes and supernatants were recovered. Equal amounts of protein extracts were resolved by SDS-PAGE on a 12% acrylamide gel and analyzed by western blot using primary antibodies for phospho-cofilin (Sigma), total cofilin (Sigma), total Cdk5 (Santa Cruz), total alpha-Pak (Santa Cruz), total LimK (Santa Cruz) and Gapdh (Millipore), followed by the corresponding IgG HRP-conjugated secondary antibody (Bio-Rad) and detected by enhanced chemiluminescence (Western Blot Luminol Reagent, Santa Cruz Biotechnology).

Gel mobility shift assays

GST-Srf and control GST proteins were purified from *Escherichia coli* cultures using standard protocols. Wild-type and mutant DNA probes were labeled with [α-^{32}P]dCTP using a Klenow fill-in method and purified using a G25 DNA purification column (Roche). The 20 μl binding reaction contained 1 μg poly(dI-dC) (Sigma), 100,000 cpm of probe, and increasing amounts (50-500 ng) of purified GST-Srf. After incubation at room temperature for 15 minutes, the reactions were separated on a 5% PAGE gel in 0.5×TBE.

Luciferase assays

The Pctaire1-luciferase construct contained the 500 bp region of *Pctaire1* containing the Srf binding site. Cos cells were plated in 24-well plates (5×10^4 cells per well) and transfected with 150 ng of the Pctaire1-luciferase construct together with 50 ng of the expression plasmids encoding myocardin and 10, 50 and 100 ng of the Srf expression plasmid using 1.4 μl of FuGENE 6 Reagent (Roche Molecular Biochemicals). Transfection efficiency was normalized by cotransfection of 10 ng pCMV-lacZ. Forty-eight hours post-transfection, the cells were harvested in 150 μl of Passive Lysate Buffer (Promega) and 20 μl of cell lysate was used for luciferase or β-galactosidase assays.

Chromatin immunoprecipitation (ChIP)

ChIP assays were performed using EZ ChIP (Millipore) following the manufacturer's instructions. Briefly, human 293T cells were transfected with either control empty vector or with flag-Srf-encoding vector. For each immunoprecipitation, chromatin from 3×10^6 cells was cross-linked with 1% formaldehyde and sonicated to produce chromatin fragments between 400 and 1000 bp. Ten percent of the chromatin was used as input control. The other 90% of the chromatin was incubated with anti-flag agarose affinity beads (Sigma). DNA was purified from the ChIP and the control input samples and analyzed by RT-PCR or by qPCR using primers spanning the predicted Srf binding site of the human *PCTAIRE1* gene.

Kinase assay

Cdk5 was immunoprecipitated from control or MRTF bdKO cortices using anti-Cdk5 antibody (Santa Cruz Biotechnology), conjugated to glutathione-agarose beads, and washed with PBS. Immunoprecipitated Cdk5 beads were then resuspended in kinase reaction buffer (30 μl) containing 12.5 μM ATP and 5 μCi of [γ-^{32}P]ATP, and recombinant histone H1 protein (100 μg). Reactions were allowed to proceed for 30 minutes at room temperature and phosphoproteins were then bound to Whatman filter papers and analyzed in a Beckman coulter counter.

Quantification of phalloidin staining

ImageQuant (Molecular Dynamics) was used to compute the integrated density or pixel density per area. A total of 30 fields of phalloidin-stained sections from three different animals were analyzed (ten fields per animal). The percentage integrated density for MRTF bdKO sections was calculated relative to control sections.

Statistical analysis

Results are expressed as mean ± s.e.m. An unpaired two-tailed Student's *t*-test with Welch correction was performed to determine statistical significance between groups. $P<0.05$ was considered significant.

RESULTS

Conditional deletion of *Mrtfa* and *Mrtfb* in the brain

To explore the potential functions of MRTFs in postnatal development, we generated a conditional null *Mrtfb* allele by homologous recombination in ES cells (Fig. 1A). Deletion of exon 8 eliminates binding to Srf, thereby allowing analysis of the influence of MRTF on Srf activity in vivo. Correct targeting and germline transmission were confirmed by Southern blot and PCR of genomic DNA (Fig. 1B,C). Specific deletion of *Mrtfb* in the brain was achieved using *GFAP-Cre* transgenic mice, which express Cre recombinase in radial glial cells as early as E12.5. Radial glial cells give rise to glial cells, to the majority of neurons in the cerebral cortex, hippocampus and cerebellum, and to adult subventricular zone (SVZ) stem cells that produce neurons throughout adult life (Zhuo et al., 2001). *Mrtfb*$^{F/F}$;*GFAP-Cre* (*Mrtfb*^{KO}) mice were phenotypically normal. Significant *Mrtfb* knockout in the brain was confirmed by RT-PCR analysis of mRNA from the cortical regions of *Mrtfb*^{KO} and *Mrtfb*^{F} mice using primers detecting exons 7, 9 and 10, which flank the deleted region of the gene. The mutant allele included exons 1 to 7. Portions of the *Mrtfb* transcript 3′ of exon 7 could not be detected in homozygous mutant embryos (Fig. 1D).

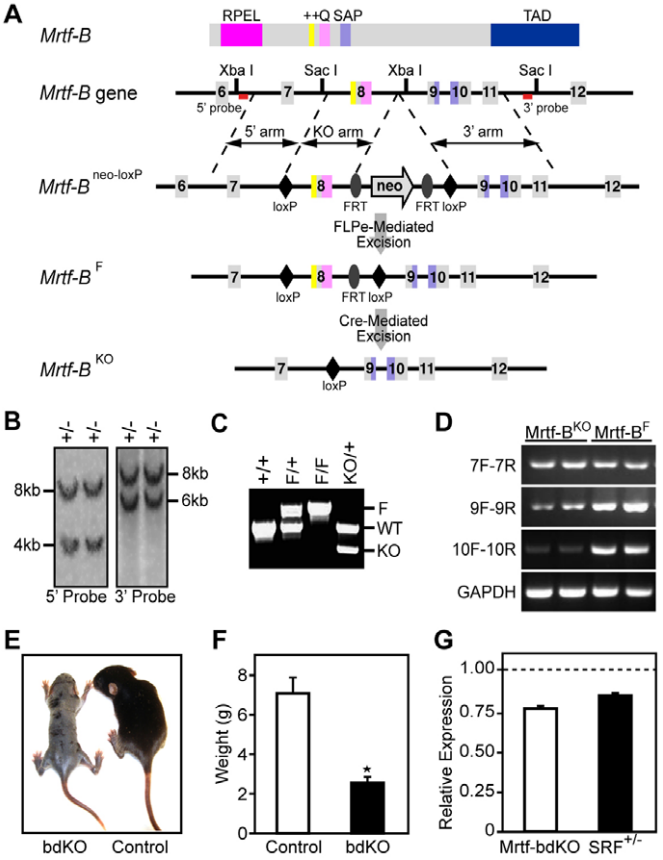

Fig. 1. Generation of MRTF brain double-knockout (bdKO) mice. (**A**) Strategy to generate a conditional *Mrtfb* allele. The protein, corresponding exonic structure, and targeted alleles are shown. The targeted *Mrtfb*$^{neo\text{-}loxP}$ allele was generated by homologous recombination in ES cells. To generate the *Mrtfb*^{F} allele, the neomycin resistance cassette, flanked by FRT sites, was removed by crossing to *FLPe* transgenic mice. The *Mrtfb*^{F} allele includes two loxP sites inserted into introns 7 and 8. The *Mrtfb*^{KO} allele was generated using Cre-mediated excision, which results in one loxP site in place of exon 8. (**B**) Southern blot analysis confirming targeting of ES cells. The corresponding wild-type (8 kb) and targeted bands (4 kb and 6 kb) are indicated for the 5′ and 3′ probes. (**C**) Genotyping of *Mrtfb*^{F} and *Mrtfb*^{KO} mice by genomic PCR. Primer set includes three primers, with two flanking the 5′ loxP site and the third downstream of the 3′ loxP site. (**D**) MRTF knockout in MRTF bdKO brains compared with control brains was assayed by RT-PCR using primers located within exons 7, 9 and 10 of *Mrtfb*. (**E**) MRTF bdKO mouse (left) and control *Mrtfa*$^{-/+}$;*Mrtfb*$^{F/F}$;*GFAP-Cre* mouse (right) at P14. Note that one copy of *Mrtfa* or *Mrtfb* is sufficient for normal development. (**F**) Average weight of control and bdKO mice at P14. The MRTF bdKO mice are significantly smaller than their control littermates. (**G**) Expression of *Srf* transcripts in MRTF bdKO brains. Shown is a quantitative RT-PCR transcript analysis from the cortical regions of MRTF bdKO and *Srf*$^{+/-}$ mice. Relative expression was normalized to the corresponding transcript levels in control brains.

Given the overlapping expression and homology between MRTF-A and MRTF-B (Pipes et al., 2006; Shiota et al., 2006), we speculated that MRTF-A could compensate for MRTF-B function in the brains of *Mrtfb*-null mice. To test this, we crossed our *Mrtfb*

conditional knockout mice to those harboring an *Mrtfa*-null (*Mrtfa*$^{-/-}$) allele (Li et al., 2006) to generate mice lacking both MRTF-A and MRTF-B in the brain. We refer to the *Mrtfa*$^{-/-}$;*Mrtfb*$^{F/F}$;*GFAP-Cre* mice as MRTF brain double-knockout (MRTF bdKO) mice.

MRTF bdKO mice were born at Mendelian ratios, but showed a significant reduction in body size and weight by P14 and died between P16 and P21 (Fig. 1E,F). *Mrtfa*$^{-/+}$;*Mrtfb*$^{F/F}$;*GFAP-Cre* and *Mrtfa*$^{-/-}$;*Mrtfb*$^{F/+}$;*GFAP-Cre* mice were phenotypically normal, suggesting that a single copy of either *Mrtfa* or *Mrtfb* is sufficient to rescue the phenotype.

Interestingly, MRTFs regulate not only Srf activity but also transcription of the *Srf* gene. Similar to MRTF deletion, ablation of Srf in the brain results in lethality by P21 (Alberti et al., 2005). Hence, we examined the expression levels of *Srf* in brains of MRTF bdKO mice. Quantitative real-time PCR (qPCR) showed a 25% reduction in the levels of *Srf* transcripts in the cortical regions of MRTF bdKO mice compared with control mice. Moreover, we compared the mRNA levels of *Srf* among MRTF bdKO mice and *Srf*$^{+/-}$ mice, which do not show an obvious brain phenotype. The levels of *Srf* were comparable between MRTF bdKO brains and *Srf*$^{+/-}$ brains; suggesting that the lethality of MRTF bdKO mice cannot be exclusively caused by downregulation of Srf at the transcriptional level (Fig. 1G).

MRTF bdKO mice have severe brain abnormalities

Histological analyses of brain sections from MRTF bdKO mice at P16 revealed several morphological abnormalities in the hippocampus, corpus callosum, anterior commissures and striatum that phenocopy defects reported in mice with brain-specific deletion of *Srf* (Alberti et al., 2005). Hematoxylin and Eosin (H&E) staining of sagittal brain sections from MRTF bdKO mice showed a reduction in the size of the striatum and an expansion of the SVZ (Fig. 2A,B). H&E staining of coronal sections from MRTF bdKO mice revealed an absence of both the corpus callosum and the anterior commissures, accompanied by a compressed hippocampus with a deformed dentate gyrus (Fig. 2C,D) (see Fig. S1 in the supplementary material). Nissl staining of hippocampal neurons identified a poorly defined pyramidal cell layer in MRTF bdKO mice (Fig. 2E,F), a phenotype that we confirmed by Golgi staining (Fig. 2G,H). Golgi staining also showed a dramatic decrease in the number of hippocampal neuronal projections compared with control neurons (Fig. 2G,H). We wondered whether the observed abnormalities in MRTF bdKO brains could be explained by glial cell defects. However, immunohistochemistry for the glial cell marker Gfap at P1 and P14 did not reveal any major differences between MRTF bdKO brain and control sections, suggesting that neuronal cell defects were most likely responsible for the observed abnormalities (see Fig. S2 in the supplementary material).

Defective neuronal migration along the rostral migratory stream

The accumulation of cells at the SVZ in MRTF bdKO brains could be observed as early as P0. Normally, newborn neurons originating from the SVZ migrate out tangentially along the rostral migratory stream (RMS) towards the olfactory bulbs, where they differentiate into interneurons (Fig. 3A). We speculated that the phenotype we observed in MRTF bdKO mice at the SVZ was due to a neuronal migration defect. This hypothesis was supported by the fact that *Mrtfa/b*-null mouse embryonic fibroblasts (MEFs) failed to arrange their cytoskeleton and migrate to the wound site in an in vitro scratch assay (see Fig. S3 in the supplementary material).

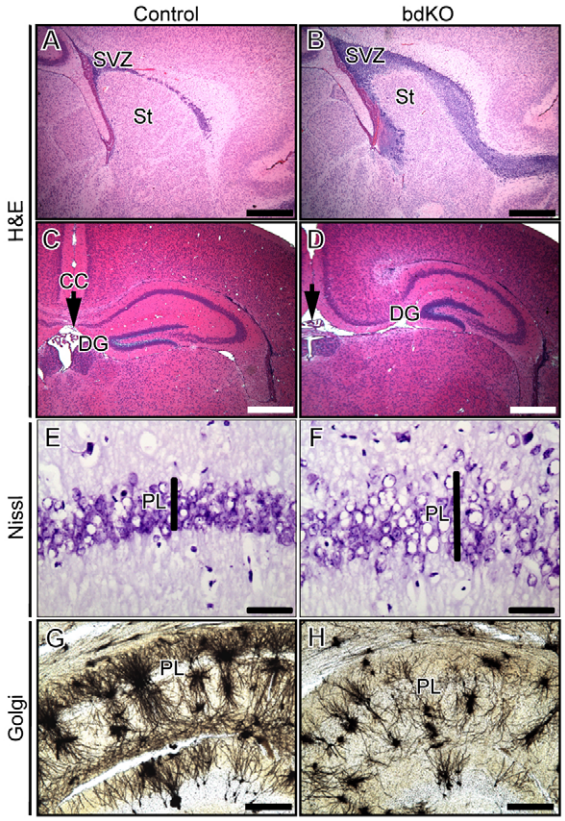

Fig. 2. Neuroanatomical defects in MRTF bdKO mice. (**A**,**B**) Hematoxylin and Eosin (H&E)-stained brain sections of control (A) and MRTF bdKO (B) brains at P16. Note the reduced striatum (St) and the broad subventricular zone (SVZ). (**C**,**D**) H&E-stained coronal brain sections of control (C) and bdKO (D) mice reveal a missing corpus callosum (CC) (arrowheads) and a deformed hippocampus with deformed dentate gyrus (DG). (**E-H**) Defective hippocampal anatomy of MRTF bdKO mice. Nissl staining reveals a loosely defined pyramidal cell layer (PL) of the hippocampi of MRTF bdKO mice (F) compared with their control littermates (E). Golgi staining reveals defects in the arrangement of the pyramidal neurons and diminished neuronal projections within the hippocampi in the MRTF bdKO brains (H) compared with control brain sections (G). Scale bars: 500 μm in A-D; 100 μm in E-H.

Alternatively, SVZ expansion could result from excessive neuron proliferation at the SVZ. To distinguish between these possibilities, we used BrdU labeling to monitor cellular proliferation and migration from the SVZ towards the olfactory bulb. BrdU pulse labeling for 1 hour at E15.5 did not reveal a difference in the rate of cell proliferation at the SVZ (see Fig. S4 in the supplementary material).

We then chased the BrdU-labeled neurons by analyzing their number and position in P7 mice. In control mice, the majority of BrdU-positive cells had migrated away from the SVZ by P7; whereas MRTF bdKO mice showed a significant accumulation of BrdU-positive cells at the SVZ (Fig. 3A,B). As a consequence of the defective neuronal migration along the RMS, the number of neurons at the olfactory bulbs in the MRTF bdKO brains was significantly diminished compared with control brains (Fig. 3C,D). These results demonstrate that the expanded SVZ we observed in MRTF bdKO mice is due to defective neuronal migration and further support the hypothesis that MRTFs regulate cytoskeletal dynamics in the developing nervous system.

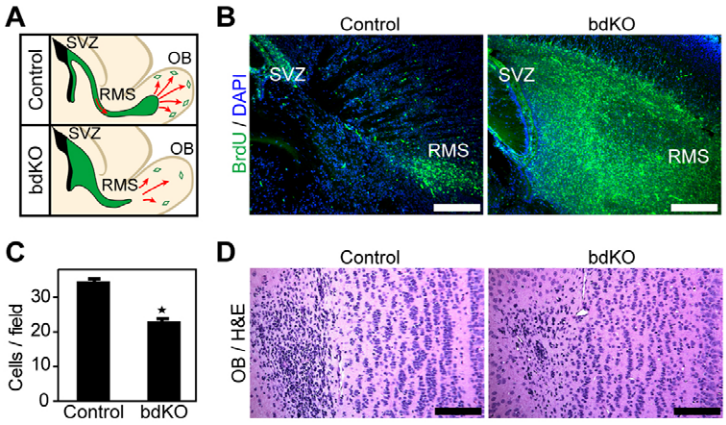

Fig. 3. Defects in neuronal cell migration from the SVZ. (**A**) Migration of neuronal precursors along the rostral migratory stream (RMS). Schematic illustrates the normal migration of cells born at the SVZ along the RMS to reach the olfactory bulbs (OB), where they differentiate into interneurons. This process is disrupted in bdKO mice, in which cells accumulate at the SVZ. (**B**) BrdU labeling shows impaired migration of neuronal cells from the SVZ along the RMS. Sagittal brain sections stained with anti-BrdU antibody reveal the accumulation of BrdU-positive cells in the SVZ of MRTF bdKO brains as compared with normal migration in the control sections. (**C**) Cell counts for neurons at the olfactory bulb in MRTF bdKO mice. Counts of the number of cells per field (40 fields total from four sections) reveal a significant difference between the number of neurons in the olfactory bulb of bdKO and control mice (**P*<0.0001). (**D**) H&E-stained brain sections at the level of the olfactory bulb show a decrease in the number of interneurons in the bdKO mice as compared with their control littermates. Scale bars: 200 μm.

Defective neurite outgrowth in MRTF bdKO neurons

In addition to defects in neuronal cell number, organization and position, we also observed by Golgi staining that the number of projections from hippocampal neurons was dramatically reduced in MRTF bdKO mice at P16 (Fig. 2H). Considering the role of the MRTF/Srf pathway in regulating cytoskeletal genes and the implication that Srf participates in neurite outgrowth (Knoll et al., 2006), we further investigated the role of MRTFs in directing neuronal projections outside the hippocampus. We performed anti-MAP2 (also known as Mtap2 – Mouse Genome Informatics) antibody staining to examine the organization of neuronal extension in vivo. Interestingly, MRTF bdKO mice showed less MAP2 in the striatum and cortical regions of the brain than control animals (Fig. 4A-D). The presence of defective neuronal projections in the cortex was also confirmed by Golgi staining (Fig. 4E,F).

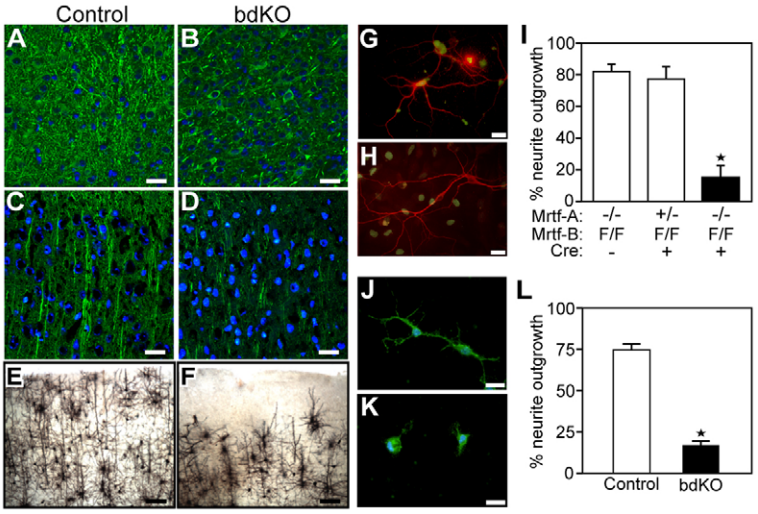

Fig. 4. Decreased neuronal projections in MRTF bdKO brains. (**A-D**) Reduced MAP2 staining in the striatum (A,B) and cortical (C,D) regions of MRTF bdKO mice at P16. Shown are anti-MAP2 antibody-stained sections of control and MRTF bdKO mice. (**E**,**F**) Defective anatomy of the cerebellar cortex of MRTF bdKO mice. Golgi staining reveals defects in the arrangement of cortical neurons and decreased neuronal projections in the MRTF bdKO brains (F) compared with control brain sections (E). (**G-I**) Hippocampal neurons derived from *Mrtfa*$^{-/+}$;*Mrtfb*$^{F/F}$ or *Mrtfa*$^{-/-}$;*Mrtfb*$^{F/F}$ mouse pups at P0-P3 were infected with either GFP-Cre-expressing (H) or control GFP-expressing (G) adenovirus. Shown are the GFP and anti-MAP2 antibody stainings from 2-week neuron cultures. (I) The percentage of GFP-positive cells that show neurite outgrowth. A significant decrease in the percentage of neurite outgrowth is seen in *Mrtfa*$^{-/-}$;*Mrtfb*$^{F/F}$ Cre-infected neurons compared with *Mrtfa*$^{-/-}$;*Mrtfb*$^{F/F}$ GFP-infected or *Mrtfa*$^{-/+}$;*Mrtfb*$^{F/F}$ Cre-infected control neurons. Forty-five fields were counted from three different experiments (**P*<0.03). (**J-L**) Neurite outgrowth in hippocampal neurons derived from MRTF bdKO or control *Mrtfa*$^{-/+}$;*Mrtfb*$^{F/F}$ mouse pups. Shown is anti-MAP2 antibody staining from 1-week neuron cultures. (L) Significant decrease in the percentage of neurite outgrowth in the bdKO culture compared with the control culture. Thirty fields were counted from three different experiments (**P*<0.001). Scale bars: 50 μm in A-D; 100 μm in E,F; 10 μm in G,H,J,K.

To confirm that the decrease in MAP2 staining is indeed indicative of a defect in neurite extension, we performed an in vitro neurite outgrowth assay in which hippocampal and cortical neurons were cultured from *Mrtfa*$^{-/-}$;*Mrtfb*$^{F/F}$ P0-P3 mice and infected with GFP-Cre-expressing adenovirus. Only ~15% of the MRTF bdKO neurons formed readily identifiable neurites over the 2-week culture period, as compared with 80% neurite outgrowth in control cultures (Fig. 4G-I). The same assay was used to examine neurite outgrowth in primary cultures of MRTF bdKO neurons over a 1-week culture period. In this assay, 75% of neurons in control cultures formed neurites, compared with less than 20% in the MRTF bdKO neuronal cultures (Fig. 4J-L). Taken together, these studies show that MRTFs induce neurite outgrowth in multiple regions of the forebrain.

Pctaire1 is a novel MRTF/Srf target gene

In order to explore the molecular basis for the abnormalities in neurite outgrowth and migration in MRTF bdKO mice, we performed microarray analysis on cortical samples from control and MRTF bdKO brains at P0 (GEO accession number GSE22117). As expected, the expression of numerous cytoskeletal components and known Srf target genes, such as gelsolin, was diminished in the MRTF bdKO mice (see Table S1 in the supplementary material). We confirmed the downregulation of beta-actin and of the actin-binding protein gelsolin in the hippocampal and cortical regions of MRTF bdKO brains by qPCR (see Fig. S5 in the supplementary material).

In addition to these known Srf target genes, we noted a small set of genes that were downregulated in the microarray, were not known Srf targets, and that function during neuronal development. Among these, *Pctaire1* (also known as *Cdk16* – Mouse Genome Informatics), which encodes a protein kinase that associates with Cdk5, was one of the most strongly downregulated genes in the microarray. Gene expression analysis by qPCR confirmed downregulation of *Pctaire1*, but not *Pctaire2* (also known as *Cdk17*), in the cortical and hippocampal regions of MRTF bdKO mice (Fig. 5A). Furthermore, anti-Pctaire1 staining revealed decreased expression of Pctaire1 in the pyramidal cells of the hippocampus and in the cortex of MRTF bdKO mice as compared with control mice (Fig. 5B).

We analyzed the DNA sequence of the *Pctaire1* gene and identified an evolutionarily conserved sequence resembling a CArG box located within the first intron (see Fig. S6 in the supplementary material). We note, however, that the site contains an additional nucleotide in the central region (CC ATTCTAT GG) that differs from the consensus CArG box sequence [CC $(A/T)_6$ GG]. Nevertheless, gel mobility shift assays showed that this sequence formed a DNA-protein complex with recombinant GST-Srf protein (Fig. 5C). Protein binding was disrupted following mutation of the CArG box and was competed by the unlabeled wild-type probe, but not by the mutated probe. Moreover, a luciferase reporter containing a 500 bp genomic DNA fragment that includes the putative CArG box was activated by Srf and myocardin in a dose-dependent manner and this activation was blunted in a reporter containing a mutated CArG box (Fig. 5D). Furthermore, we performed chromatin immunoprecipitation (ChIP) and were able to detect binding of flag-tagged Srf to its predicted Srf binding site in *PCTAIRE1* in the context of native chromatin in human 293T cells (Fig. 5E). qPCR showed a ~10-fold enrichment of Srf binding as compared with background binding (Fig. 5F).

These findings suggested that Pctaire1 might function as an essential effector of the Srf/MRTF pathway during neurite outgrowth. Confirming the potential influence of Pctaire1 on

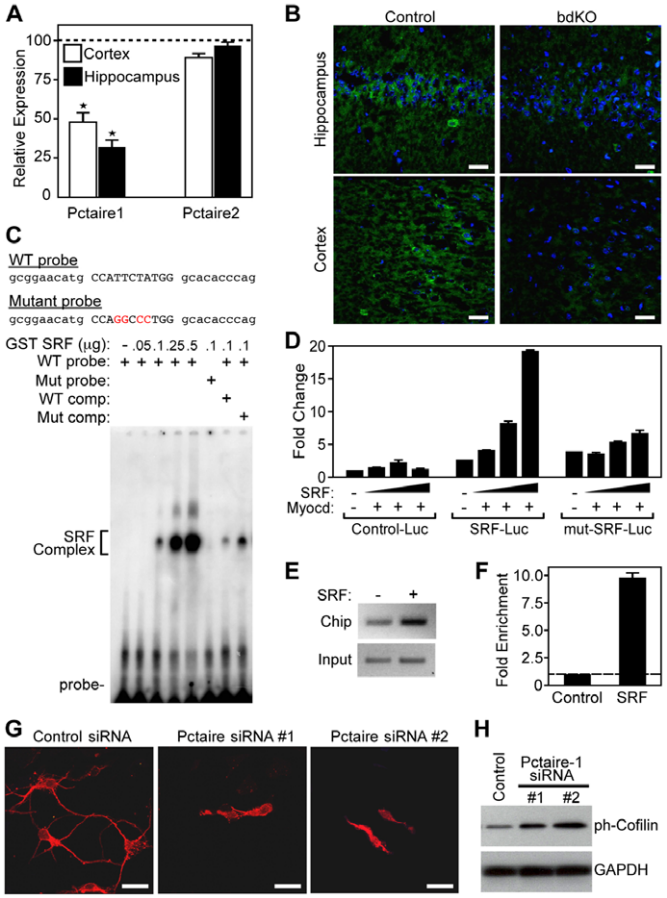

Fig. 5. Identification of *Pctaire1* as a novel MRTF/Srf target gene. (**A**) Decreased expression of *Pctaire1* transcripts in MRTF bdKO brains. Quantitative RT-PCR transcript analysis from hippocampal and cortical regions of MRTF bdKO brains. Relative expression was normalized to the corresponding transcript levels in control brains. **P*<0.05. (**B**) Diminished levels of Pctaire1 protein in MRTF bdKO brains. Anti-Pctaire1 antibody staining revealed decreased levels of the protein in the hippocampal and cortical regions of MRTF bdKO mice compared with control mice. (**C**) Gel mobility shift assays were performed with a labeled *Pctaire1* probe and purified GST-Srf or control GST proteins. Increased binding of GST-Srf to the *Pctaire1* CArG sequence was detected with increased amounts of recombinant Srf. The use of a labeled mutant probe or an unlabeled probe blocks Srf binding. (**D**) Responsiveness of *Pctaire1* expression to MRTF/Srf signaling. Increased amounts of the Srf were able to activate the Pctaire1-luciferase reporter constructs containing the predicted Srf binding site but not the empty luciferase constructs. Mutation of the predicted CArG box blocks this activation. (**E**,**F**) Enrichment of Srf at its predicted binding site within the *PCTAIRE1* gene. ChIP assay were performed on chromatin prepared from human 293T cells transfected with either a flag-tagged Srf construct or a control empty construct. The precipitated genomic DNA was analyzed by RT-PCR (E) and by qPCR (F) using primers for the human *PCTAIRE1* gene. Shown also is the PCR amplification performed prior to immunoprecipitation as the input control (E). (**G**) Defective neurite outgrowth in Pctaire1 knockdown neurons. Anti-MAP2 antibody staining from 1-week neuron cultures shows disruption of neurite outgrowth in the Pctaire1 siRNA-transfected but not in control siRNA-transfected neurons. (**H**) Increased cofilin phosphorylation in Pctaire1 knockdown neurons. Western blot analysis of phospho-cofilin and total cofilin in control and Pctaire1 siRNA-transfected neurons. Gapdh was used as a loading control. Scale bars: 50 μm in B; 5 μm in G.

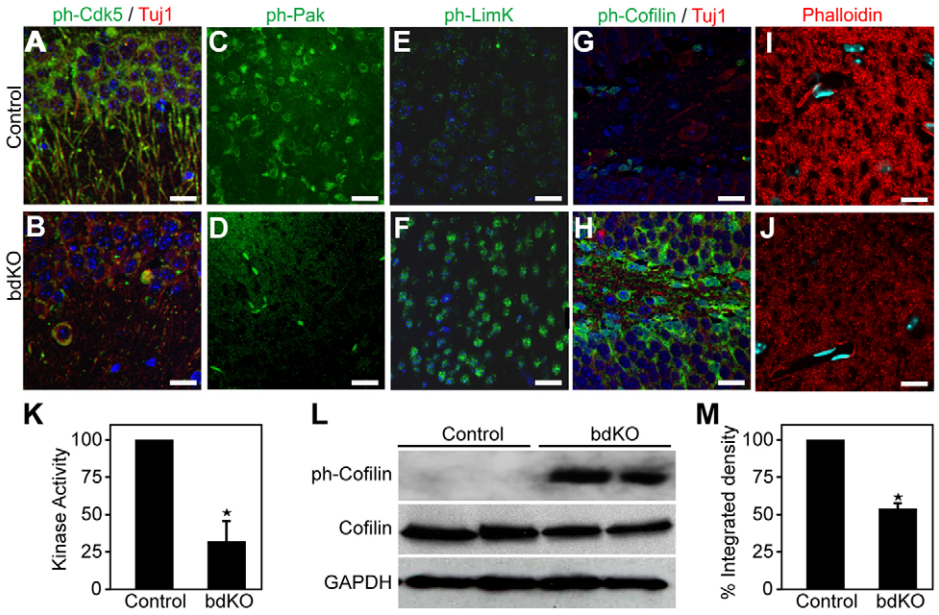

Fig. 6. Regulation of actin dynamics by the MRTF/Srf pathway. (**A-H**) Dysregulation of phosphorylated (ph) Cdk5, LimK and cofilin in MRTF bdKO brains. Anti-ph-Cdk5 (A,B), anti-ph-Pak (C,D), anti-ph-LimK (E,F), and anti-ph-cofilin (G,H) staining revealed decreased phosphorylation of Cdk5 and increased phosphorylation of LimK and cofilin in the brains of MRTF bdKO mice (B,D,F,H) as compared with control mice (A,C,E,G). (**I**,**J**) Decreased actin polymerization in the MRTF bdKO brain. Phalloidin staining revealed decreased levels of F-actin in the hippocampal regions of MRTF bdKO mice (J) compared with control mice (I). Scale bars: 50 μm. (**K**) Diminished kinase activity of Cdk5 upon MRTF deletion. Kinase assays show a ~75% decrease in the kinase activity of Cdk5 immunoprecipitated from the brains of MRTF bdKO mice compared with control mice. **P*<0.05. (**L**) Western blot analysis of phospho-cofilin and total cofilin in the cerebellar cortex of control and MRTF bdKO brain samples. Gapdh was used as a loading control. (**M**) Quantification of F-actin levels in MRTF bdKO mice. Shown is the percentage integrated density (pixel density per area) of the phalloidin-stained MRTF bdKO cortical sections normalized to control sections. **P*<0.05.

neuronal cell morphology and neurite outgrowth, knockdown of Pctaire1 using two different siRNAs in primary neuron cultures disrupted neurite outgrowth, phenocopying MRTF bdKO neuronal cultures (Fig. 5G).

Regulation of actin dynamics by MRTFs

Pctaire1 has been reported to interact with Cdk5, a kinase implicated in actin dynamics and neurite outgrowth (Cheng et al., 2002). To assess the potential impact of MRTF signaling on Cdk5 activity, we performed immunohistochemistry against the activated (phosphorylated) form of Cdk5 and observed reduced phospho-Cdk5 accumulation in the hippocampal and cortical regions of MRTF bdKO mice compared with control littermates, with no significant reduction in the total Cdk5 levels (Fig. 6A,B and see Fig. S7 in the supplementary material; data not shown). To further confirm the abrogated activity of Cdk5 in MRTF bdKO brains, we performed a Cdk5 kinase assay with immunoprecipitated Cdk5 from the cortical regions of control or MRTF bdKO mice and used recombinant histone H1 protein as substrate. Indeed, the kinase activity of Cdk5 was significantly reduced in the MRTF bdKO brains as compared with control brains (Fig. 6K).

Cdk5 regulates neuronal migration and neurite outgrowth by modulating the activity of a kinase cascade that targets actin polymerization (Dhavan and Tsai, 2001; Smith, 2003). At the base of this cascade is the actin depolymerase cofilin, the activity of which is diminished by phosphorylation (Kuhn et al., 2000; Sarmiere and Bamburg, 2004). Cofilin is a substrate for LIM kinase (LimK), which in turn is a substrate for the kinase Pak1 (Arber et al., 1998). Cdk5 inactivates Pak1 via phosphorylation and promotes actin depolymerization. We speculated that the Pak1-LimK-cofilin cascade is a target of Cdk5 downstream of MRTFs. Indeed, the cortical and hippocampal regions of the MRTF bdKO mice showed diminished Pak phosphorylation and a greater accumulation of phospho-LimK and phospho-cofilin than control brains (Fig. 6C-H; data not shown). Furthermore, immunoblotting for phospho-cofilin and total cofilin showed a dramatic increase in phospho-cofilin in the brains of MRTF bdKO mice compared with controls, without a significant change in total levels of cofilin protein (Fig. 6L and see Fig. S5 in the supplementary material). The total levels of Pak and LimK were unchanged (see Fig. S7 in the supplementary material). Interestingly, the levels of phospho-cofilin were also increased upon knockdown of Pctaire1 in primary neuronal cultures, further supporting our model and placing Pctaire1 as an upstream regulator of cofilin phosphorylation in the brain (Fig. 5H). These results define a mechanistic pathway in which MRTFs induce Pctaire1 and Cdk5 activity, which in turn inactivate the Pak1-Limk cascade to promote the actin-depolymerizing activity of cofilin and neuronal outgrowth.

To verify that MRTF deletion results in dysregulation of actin severing and abrogates actin dynamics, we evaluated the levels of actin polymerization by F-actin staining with phalloidin. Phalloidin staining of *Mrtfa/b*-null MEFs showed actin cytoskeleton disruptions and a lack of cortical accumulation of actin filaments upon MRTF deletion in MEFs (see Fig. S8 in the supplementary material). The levels of F-actin were also markedly decreased in the cortical and hippocampal regions of MRTF bdKO mice compared with their control littermates (Fig. 6I,J). Quantification

of phalloidin staining showed ~50% reduction in the levels of F-actin in MRTF bdKO sections compared with control sections (Fig. 6M). MRTFs are thus essential regulators of actin dynamics in neurons.

DISCUSSION

The results of this study reveal obligate roles for MRTF-A and MRTF-B as redundant regulators of neurite outgrowth and neuronal migration during brain development in vivo. The abnormalities in brain development resulting from the combined deletion of *Mrtfa* and *Mrtfb* reflect disorganization of the actin cytoskeleton and impairment of actin dynamics. MRTFs couple the Rho and Cdk5 signaling pathways to actin treadmilling and Srf-dependent transcription to regulate neuronal development, as schematized in Fig. 7. Targets of the MRTF/Srf signaling pathway include genes that encode actin and other cytoskeletal components, as well as *Pctaire1*, a negative regulator of actin polymerization. MRTFs also promote the kinase activity of a second negative regulator of actin polymerization, Cdk5, probably at the post-transcriptional level. Thus, MRTFs function as nodal regulators that couple two downstream signaling pathways that modulate cytoskeletal dynamics, thereby fulfilling a cytoskeletal-transcriptional circuit that governs neurite outgrowth and neuronal development.

Functions of MRTFs in vivo

This study is the first to reveal the importance of the MRTF/Srf partnership during brain development in vivo. Potentiation of the transcriptional activity of Srf by MRTFs has been well documented in vitro (Pipes et al., 2006). However, the phenotypes of knockout mice lacking myocardin, *Mrtfa* or *Mrtfb* have not been comparable to those of *Srf* knockout mice. The remarkable similarities between the neuronal defects resulting from deletion of both *Mrtfa* and *Mrtfb* and those reported for brain-specific *Srf* knockout mice (Alberti et al., 2005; Knoll et al., 2006) strongly suggest that the actions of Srf in the brain rely completely on its association with MRTFs and argue against the involvement of other transcriptional co-factors in mediating Srf signaling during brain development. The redundancy of MRTF functions in the brain contrasts with the distinct phenotypes observed in *Mrtfa* and *Mrtfb* single-knockout mice (Li et al., 2005; Li et al., 2006; Oh et al., 2005; Sun et al., 2006). Interestingly, neuronal defects were only observed upon deletion of all four MRTF alleles in the brain.

MRTFs as regulators of actin cytoskeleton dynamics

Precise control of the neuronal actin cytoskeleton governs multiple events during brain development, such as neurite outgrowth and neuronal migration. Such control could be exerted by direct regulation of the expression of G-actin and by regulation of the activity of actin-binding proteins, which influence actin dynamics. In a recent report, Stern et al. made use of several actin mutants to show that actin filaments can induce neurite outgrowth in neuronal cultures and that regulation of neurite length by actin filaments is mediated by the activity of Srf (Stern et al., 2009). Our finding that deletion of *Mrtfa* and *Mrtfb* disrupts the assembly of actin filaments accounts for the defective neuronal migration and neurite outgrowth in the brains of MRTF bdKO mice.

Genetic ablation of MRTF-A and MRTF-B also results in decreased expression and activity of the two major actin-severing proteins gelsolin and cofilin. Unlike gelsolin, which does not require phosphorylation for activity, the actin-severing activity of cofilin is inhibited through phosphorylation by LIM kinases (Kuhn et al., 2000; Sarmiere and Bamburg, 2004). Interestingly, gelsolin and cofilin are also dysregulated following deletion of *Srf* in the brain (Alberti et al., 2005), further supporting the role of MRTFs as essential Srf activators. Both proteins are enriched at growth cones and are required to maintain a high concentration of G-actin for continued actin polymerization during cell migration and neurite outgrowth (Cunningham et al., 1991; Furnish et al., 2001; Gurniak et al., 2005; Meberg, 2000; Meberg and Bamburg, 2000). Interestingly, rather than increasing actin filament assembly, the striking phosphorylation and inactivation of cofilin in our MRTF bdKO mice were accompanied by diminished actin polymerization. This observation is not surprising because, in addition to promoting actin depolymerization, cofilin has been shown to promote the assembly of actin filaments in certain cellular contexts (Chan et al., 2000; Ghosh et al., 2004; Zebda et al., 2000). Recent mechanisms addressing cofilin function propose that the actin-severing activity of cofilin creates new barbed ends, which are used to nucleate polymerization of new actin filaments. Therefore, aberrant actin severing could explain the defective organization of the actin cytoskeleton in the brains MRTF bdKO mice.

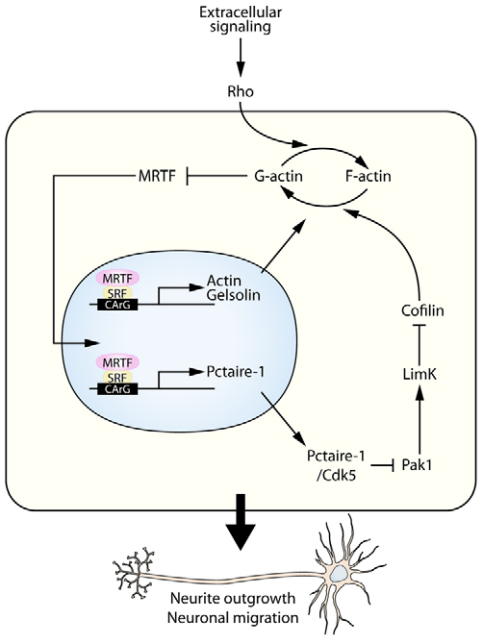

Fig. 7. Model for the regulation of neuronal migration and neurite outgrowth by the MRTF/Srf pathway. MRTFs are essential mediators of Srf signaling in the mouse brain and key regulators of the dynamics of the actin cytoskeleton. Together with Srf, MRTFs regulate the expression of β-actin and other actin-binding proteins, such as gelsolin. In addition, activation of MRTF/Srf signaling regulates the expression of the Pctaire1 kinase, which is involved in the regulation of neurite outgrowth. Under normal conditions, the MRTF/Srf pathway regulates the activity of Cdk5, which phosphorylates and inactivates Pak1. Decreased Pak1 activity results in diminished LimK activity towards phosphorylation of cofilin, resulting in increased actin severing. Genetic ablation of MRTFs in the mouse brain disrupts actin dynamics by disrupting the expression and/or activity of actin and the actin-severing proteins gelsolin and cofilin, resulting in defective neuronal migration and neurite outgrowth.

Identification of Pctaire1 as a novel MRTF/Srf target gene in the brain

We show that the MRTF/Srf pathway regulates Pctaire1 kinase in the brain. Pctaire1 is an atypical Cdc-like kinase in that it does not require cyclins for activation and is not involved in cell cycle regulation (Besset et al., 1998; Graeser et al., 2002; Okuda et al., 1992). It is expressed at low levels in most cell types, but is particularly abundant in postmitotic neurons (Besset et al., 1999). Two lines of evidence link Pctaire1 function in neurons to the regulation of neurite outgrowth, the first showing regulation of neurite outgrowth by Pctaire1 in Neuro-2a cells (Graeser et al., 2002) and the second reporting the interaction between Pctaire1 and the Cdk5 pathway (Cheng et al., 2002), which is implicated in the regulation of neuronal actin dynamics. We show here that MRTF/Srf activates *Pctaire1* expression through a CArG-like box within the first intron of the gene, and that knockdown of Pctaire1 blocks the growth of neurites in primary neuron cultures, mimicking the effect of MRTF deletion.

Cdk5 kinase drives neuronal differentiation, actin remodeling, neuronal migration and neurite outgrowth (Dhavan and Tsai, 2001). Cdk5 phosphorylates and inhibits Pak1, linking the activity of Cdk5 to the regulation of the actin cytoskeleton (Dhavan and Tsai, 2001; Smith, 2003). Pak1 increases the phosphorylation activity of LimK towards cofilin, which blocks its depolymerizing activity and thereby inhibits actin turnover (Arber et al., 1998; Yang et al., 1998). Interestingly, we show that genetic deletion of MRTF-A and MRTF-B in the mouse brain disrupts this cascade of protein kinases, resulting in inactivation of cofilin.

Overall, our findings and those of others demonstrate the essential role of the MRTF/Srf signaling system in the coupling of cytoskeletal dynamics to nuclear gene transcription in the nervous system. Given the importance of MRTF/Srf in the control of cytoskeletal gene expression in other cell types, especially muscle cells, it will be interesting to determine whether the Pctaire1/Cdk5 pathway identified in this study also modulates the actin cytoskeleton downstream of MRTF/Srf in other cell types.

Acknowledgements

We are grateful to Michael Haberland for his insights and comments and to Alfred Nordheim for kindly providing the *Srf* knockout mice. Work in the laboratory of E.N.O. was supported by grants from the NIH, the Donald W. Reynolds Center for Clinical Cardiovascular Research, the American Heart Association, the Robert A. Welch foundation and the Leducq Foundation. Deposited in PMC for release after 12 months.

Competing interests statement

The authors declare no competing financial interests.

Supplementary material

Supplementary material for this article is available at
http://dev.biologists.org/lookup/suppl/doi:10.1242/dev.047605/-/DC1

References

Ahlemeyer, B. and Baumgart-Vogt, E. (2005). Optimized protocols for the simultaneous preparation of primary neuronal cultures of the neocortex, hippocampus and cerebellum from individual newborn (P0.5) C57Bl/6J mice. *J. Neurosci. Methods* **149**, 110-120.

Alberti, S., Krause, S. M., Kretz, O., Philippar, U., Lemberger, T., Casanova, E., Wiebel, F. F., Schwarz, H., Frotscher, M., Schutz, G. et al. (2005). Neuronal migration in the murine rostral migratory stream requires serum response factor. *Proc. Natl. Acad. Sci. USA* **102**, 6148-6153.

Arber, S., Barbayannis, F. A., Hanser, H., Schneider, C., Stanyon, C. A., Bernard, O. and Caroni, P. (1998). Regulation of actin dynamics through phosphorylation of cofilin by LIM-kinase. *Nature* **393**, 805-809.

Arsenian, S., Weinhold, B., Oelgeschlager, M., Ruther, U. and Nordheim, A. (1998). Serum response factor is essential for mesoderm formation during mouse embryogenesis. *EMBO J.* **17**, 6289-6299.

Ayala, R., Shu, T. and Tsai, L. H. (2007). Trekking across the brain: the journey of neuronal migration. *Cell* **128**, 29-43.

Benitez-King, G., Ramirez-Rodriguez, G., Ortiz, L. and Meza, I. (2004). The neuronal cytoskeleton as a potential therapeutical target in neurodegenerative diseases and schizophrenia. *Curr. Drug Targets CNS Neurol. Disord.* **3**, 515-533.

Besset, V., Rhee, K. and Wolgemuth, D. J. (1998). The identification and characterization of expression of Pftaire-1, a novel Cdk family member, suggest its function in the mouse testis and nervous system. *Mol. Reprod. Dev.* **50**, 18-29.

Besset, V., Rhee, K. and Wolgemuth, D. J. (1999). The cellular distribution and kinase activity of the Cdk family member Pctaire1 in the adult mouse brain and testis suggest functions in differentiation. *Cell Growth Differ.* **10**, 173-181.

Chan, A. Y., Bailly, M., Zebda, N., Segall, J. E. and Condeelis, J. S. (2000). Role of cofilin in epidermal growth factor-stimulated actin polymerization and lamellipod protrusion. *J. Cell Biol.* **148**, 531-542.

Charvet, C., Houbron, C., Parlakian, A., Giordani, J., Lahoute, C., Bertrand, A., Sotiropoulos, A., Renou, L., Schmitt, A., Melki, J. et al. (2006). New role for serum response factor in postnatal skeletal muscle growth and regeneration via the interleukin 4 and insulin-like growth factor 1 pathways. *Mol. Cell. Biol.* **26**, 6664-6674.

Cheng, K., Li, Z., Fu, W. Y., Wang, J. H., Fu, A. K. and Ip, N. Y. (2002). Pctaire1 interacts with p35 and is a novel substrate for Cdk5/p35. *J. Biol. Chem.* **277**, 31988-31993.

Cunningham, C. C., Stossel, T. P. and Kwiatkowski, D. J. (1991). Enhanced motility in NIH 3T3 fibroblasts that overexpress gelsolin. *Science* **251**, 1233-1236.

Dhavan, R. and Tsai, L. H. (2001). A decade of CDK5. *Nat. Rev. Mol. Cell Biol.* **2**, 749-759.

Etkin, A., Alarcon, J. M., Weisberg, S. P., Touzani, K., Huang, Y. Y., Nordheim, A. and Kandel, E. R. (2006). A role in learning for SRF: deletion in the adult forebrain disrupts LTD and the formation of an immediate memory of a novel context. *Neuron* **50**, 127-143.

Furnish, E. J., Zhou, W., Cunningham, C. C., Kas, J. A. and Schmidt, C. E. (2001). Gelsolin overexpression enhances neurite outgrowth in PC12 cells. *FEBS Lett.* **508**, 282-286.

Ghosh, M., Song, X., Mouneimne, G., Sidani, M., Lawrence, D. S. and Condeelis, J. S. (2004). Cofilin promotes actin polymerization and defines the direction of cell motility. *Science* **304**, 743-746.

Graeser, R., Gannon, J., Poon, R. Y., Dubois, T., Aitken, A. and Hunt, T. (2002). Regulation of the CDK-related protein kinase PCTAIRE-1 and its possible role in neurite outgrowth in Neuro-2A cells. *J. Cell Sci.* **115**, 3479-3490.

Guettler, S., Vartiainen, M. K., Miralles, F., Larijani, B. and Treisman, R. (2008). RPEL motifs link the serum response factor cofactor MAL but not myocardin to Rho signaling via actin binding. *Mol. Cell. Biol.* **28**, 732-742.

Gurniak, C. B., Perlas, E. and Witke, W. (2005). The actin depolymerizing factor n-cofilin is essential for neural tube morphogenesis and neural crest cell migration. *Dev. Biol.* **278**, 231-241.

Knoll, B., Kretz, O., Fiedler, C., Alberti, S., Schutz, G., Frotscher, M. and Nordheim, A. (2006). Serum response factor controls neuronal circuit assembly in the hippocampus. *Nat. Neurosci.* **9**, 195-204.

Kuhn, T. B., Meberg, P. J., Brown, M. D., Bernstein, B. W., Minamide, L. S., Jensen, J. R., Okada, K., Soda, E. A. and Bamburg, J. R. (2000). Regulating actin dynamics in neuronal growth cones by ADF/cofilin and rho family GTPases. *J. Neurobiol.* **44**, 126-144.

Kuwahara, K., Barrientos, T., Pipes, G. C., Li, S. and Olson, E. N. (2005). Muscle-specific signaling mechanism that links actin dynamics to serum response factor. *Mol. Cell. Biol.* **25**, 3173-3181.

Lambert de Rouvroit, C. and Goffinet, A. M. (2001). Neuronal migration. *Mech. Dev.* **105**, 47-56.

Latasa, M. U., Couton, D., Charvet, C., Lafanechere, A., Guidotti, J. E., Li, Z., Tuil, D., Daegelen, D., Mitchell, C. and Gilgenkrantz, H. (2007). Delayed liver regeneration in mice lacking liver serum response factor. *Am. J. Physiol. Gastrointest. Liver Physiol.* **292**, G996-G1001.

Li, J., Zhu, X., Chen, M., Cheng, L., Zhou, D., Lu, M. M., Du, K., Epstein, J. A. and Parmacek, M. S. (2005). Myocardin-related transcription factor B is required in cardiac neural crest for smooth muscle differentiation and cardiovascular development. *Proc. Natl. Acad. Sci. USA* **102**, 8916-8921.

Li, S., Chang, S., Qi, X., Richardson, J. A. and Olson, E. N. (2006). Requirement of a myocardin-related transcription factor for development of mammary myoepithelial cells. *Mol. Cell. Biol.* **26**, 5797-5808.

Lin, L., Lesnick, T. G., Maraganore, D. M. and Isacson, O. (2009). Axon guidance and synaptic maintenance: preclinical markers for neurodegenerative disease and therapeutics. *Trends Neurosci.* **32**, 142-149.

Meberg, P. J. (2000). Signal-regulated ADF/cofilin activity and growth cone motility. *Mol. Neurobiol.* **21**, 97-107.

Meberg, P. J. and Bamburg, J. R. (2000). Increase in neurite outgrowth mediated by overexpression of actin depolymerizing factor. *J. Neurosci.* **20**, 2459-2469.

Miano, J. M., Ramanan, N., Georger, M. A., de Mesy Bentley, K. L., Emerson, R. L., Balza, R. O., Jr, Xiao, Q., Weiler, H., Ginty, D. D. and Misra, R. P.

(2004). Restricted inactivation of serum response factor to the cardiovascular system. *Proc. Natl. Acad. Sci. USA* **101**, 17132-17137.
Miralles, F., Posern, G., Zaromytidou, A. I. and Treisman, R. (2003). Actin dynamics control SRF activity by regulation of its coactivator MAL. *Cell* **113**, 329-342.
Niu, Z., Yu, W., Zhang, S. X., Barron, M., Belaguli, N. S., Schneider, M. D., Parmacek, M., Nordheim, A. and Schwartz, R. J. (2005). Conditional mutagenesis of the murine serum response factor gene blocks cardiogenesis and the transcription of downstream gene targets. *J. Biol. Chem.* **280**, 32531-32538.
Oh, J., Richardson, J. A. and Olson, E. N. (2005). Requirement of myocardin-related transcription factor-B for remodeling of branchial arch arteries and smooth muscle differentiation. *Proc. Natl. Acad. Sci. USA* **102**, 15122-15127.
Okuda, T., Cleveland, J. L. and Downing, J. R. (1992). PCTAIRE-1 and PCTAIRE-3, two members of a novel cdc2/CDC28-related protein kinase gene family. *Oncogene* **7**, 2249-2258.
Olson, E. N. and Nordheim, A. (2010). Linking actin dynamics and gene transcription to drive cellular motile functions. *Nat. Rev. Mol. Cell Biol.* **11**, 353-365.
Park, H. T., Wu, J. and Rao, Y. (2002). Molecular control of neuronal migration. *BioEssays* **24**, 821-827.
Parlakian, A., Charvet, C., Escoubet, B., Mericskay, M., Molkentin, J. D., Gary-Bobo, G., De Windt, L. J., Ludosky, M. A., Paulin, D., Daegelen, D. et al. (2005). Temporally controlled onset of dilated cardiomyopathy through disruption of the SRF gene in adult heart. *Circulation* **112**, 2930-2939.
Pipes, G. C., Creemers, E. E. and Olson, E. N. (2006). The myocardin family of transcriptional coactivators: versatile regulators of cell growth, migration, and myogenesis. *Genes Dev.* **20**, 1545-1556.
Posern, G., Miralles, F., Guettler, S. and Treisman, R. (2004). Mutant actins that stabilise F-actin use distinct mechanisms to activate the SRF coactivator MAL. *EMBO J.* **23**, 3973-3983.
Ramanan, N., Shen, Y., Sarsfield, S., Lemberger, T., Schutz, G., Linden, D. J. and Ginty, D. D. (2005). SRF mediates activity-induced gene expression and synaptic plasticity but not neuronal viability. *Nat. Neurosci.* **8**, 759-767.
Rossi, F., Gianola, S. and Corvetti, L. (2007). Regulation of intrinsic neuronal properties for axon growth and regeneration. *Prog. Neurobiol.* **81**, 1-28.
Sarmiere, P. D. and Bamburg, J. R. (2004). Regulation of the neuronal actin cytoskeleton by ADF/cofilin. *J. Neurobiol.* **58**, 103-117.
Shiota, J., Ishikawa, M., Sakagami, H., Tsuda, M., Baraban, J. M. and Tabuchi, A. (2006). Developmental expression of the SRF co-activator MAL in brain: role in regulating dendritic morphology. *J. Neurochem.* **98**, 1778-1788.
Smith, D. (2003). Cdk5 in neuroskeletal dynamics. *Neurosignals* **12**, 239-251.
Spalice, A., Parisi, P., Nicita, F., Pizzardi, G., Del Balzo, F. and Iannetti, P. (2009). Neuronal migration disorders: clinical, neuroradiologic and genetics aspects. *Acta Paediatr.* **98**, 421-433.
Stern, S., Debre, E., Stritt, C., Berger, J., Posern, G. and Knoll, B. (2009). A nuclear actin function regulates neuronal motility by serum response factor-dependent gene transcription. *J. Neurosci.* **29**, 4512-4518.
Sun, Y., Boyd, K., Xu, W., Ma, J., Jackson, C. W., Fu, A., Shillingford, J. M., Robinson, G. W., Hennighausen, L., Hitzler, J. K. et al. (2006). Acute myeloid leukemia-associated Mkl1 (Mrtf-a) is a key regulator of mammary gland function. *Mol. Cell. Biol.* **26**, 5809-5826.
Tanaka, D. H., Yamauchi, K. and Murakami, F. (2008). Guidance mechanisms in neuronal and axonal migration. *Brain Nerve* **60**, 405-413.
Vartiainen, M. K., Guettler, S., Larijani, B. and Treisman, R. (2007). Nuclear actin regulates dynamic subcellular localization and activity of the SRF cofactor MAL. *Science* **316**, 1749-1752.
Verrotti, A., Spalice, A., Ursitti, F., Papetti, L., Mariani, R., Castronovo, A., Mastrangelo, M. and Iannetti, P. (2009). New trends in neuronal migration disorders. *Eur. J. Paediatr. Neurol.* **14**, 1-12.
Wang, D., Chang, P. S., Wang, Z., Sutherland, L., Richardson, J. A., Small, E., Krieg, P. A. and Olson, E. N. (2001). Activation of cardiac gene expression by myocardin, a transcriptional cofactor for serum response factor. *Cell* **105**, 851-862.
Wang, D. Z., Li, S., Hockemeyer, D., Sutherland, L., Wang, Z., Schratt, G., Richardson, J. A., Nordheim, A. and Olson, E. N. (2002). Potentiation of serum response factor activity by a family of myocardin-related transcription factors. *Proc. Natl. Acad. Sci. USA* **99**, 14855-14860.
Yang, N., Higuchi, O., Ohashi, K., Nagata, K., Wada, A., Kangawa, K., Nishida, E. and Mizuno, K. (1998). Cofilin phosphorylation by LIM-kinase 1 and its role in Rac-mediated actin reorganization. *Nature* **393**, 809-812.
Zebda, N., Bernard, O., Bailly, M., Welti, S., Lawrence, D. S. and Condeelis, J. S. (2000). Phosphorylation of ADF/cofilin abolishes EGF-induced actin nucleation at the leading edge and subsequent lamellipod extension. *J. Cell Biol.* **151**, 1119-1128.
Zhuo, L., Theis, M., Alvarez-Maya, I., Brenner, M., Willecke, K. and Messing, A. (2001). hGFAP-cre transgenic mice for manipulation of glial and neuronal function in vivo. *Genesis* **31**, 85-94.

Table S1. Microarray data on MRTF cortical bdKO samples at P0

Fold change	Gene symbol	Gene title
–7.6	*Antxr2*	anthrax toxin receptor 2
–6.9	*Mett5d1*	methyltransferase 5 domain containing 1
–6.8	*Pctk1*	PCTAIRE-motif protein kinase 1
–6.8	*Pip5k2b*	phosphatidylinositol-4-phosphate 5-kinase II beta
–4.3	*Xmr*	Xmr protein
–3.8	*Rasef*	RAS and EF hand domain containing
–3.2	*Oog3*	oogenesin 3
–3	*Ctnna1*	catenin, alpha 1
–2.8	*Trat1*	T cell receptor associated transmembrane 1
–2.8	*Defb11*	defensin beta 11
–2.5	*Cryga*	crystallin, gamma A
–2.4	*Slc45a3*	solute carrier family 45, member 3
–2.4	*Dleu2*	deleted in lymphocytic leukemia, 2
–2.4	*Arl14*	ADP-ribosylation factor-like 14
–2.3	*Ang4*	angiogenin, ribonuclease A family, member 4
–2.3	*Kif23*	kinesin family member 23
–2.2	*Wnt3a*	wingless-related MMTV integration site 3A
–2.1	*Ctsw*	cathepsin W
–2.1	*Abcd2*	ATP-binding cassette, family D, member 2
–2	*Ccnb3*	cyclin B3
–1.9	*Jmy*	junction-mediating and regulatory protein
–1.8	*Gsn*	gelsolin
–1.8	*Sema3b*	semaphorin 3B
–1.6	*Dnase1l3*	deoxyribonuclease 1-like 3
–1.6	*Zpbp*	zona pellucida binding protein
–1.6	*Tssk6*	testis-specific serine kinase 6
–1.6	*Xlr4b*	X-linked lymphocyte-regulated 4B
–1.5	*Myh2*	myosin heavy polypeptide 2
–1.5	*Klrb1b*	killer cell lectin-like receptor b member 1B
–1.5	*Map2k7*	mitogen activated protein kinase kinase 7
–1.5	*Sema5a*	semaphorin 5A
–1.5	*Arhgef16*	Rho guanine nucleotide exchange factor16
–1.5	*Arc*	activity regulated cytoskeletal-associated protein
–1.5	*Actn1*	actinin, alpha 1
–1.5	*App*	amyloid beta (A4) precursor protein

The top 35 known genes that were expressed above background level in the control samples and were significantly downregulated in the array.